Journal of Alloys and Compounds 517 (2012) 92–97

Contents lists available at SciVerse ScienceDirect

Journal of Alloys and Compounds

journal homepage: www.elsevier.com/locate/jallcom

Oxidation protection of Sm_2Co_{17}-based alloys

W.M. Pragnell, H.E. Evans*, A.J. Williams[1]

School of Metallurgy and Materials, The University of Birmingham, Birmingham B15 2TT, UK

ARTICLE INFO

Article history:
Received 24 May 2011
Received in revised form
30 November 2011
Accepted 11 December 2011
Available online 20 December 2011

Keywords:
SmCo
Permanent magnet
High temperature oxidation
Oxidation protection
Coatings

ABSTRACT

SmCo alloys form the basis of excellent permanent magnets with potential service applications up to 550 °C. However, the rapid growth of an internal oxidation zone limits their usefulness because the accompanying microstructural changes destroy the alloys' high-temperature magnetic properties within this zone. In this work, a high-temperature grade of a $Sm_2(Co,Fe,Cu,Zr)_{17}$-based alloy was treated with a variety of potentially protective coating systems and then oxidised in air at temperatures of 450 and 550 °C to assess their performance. It was found that a diffused Pt coating and a paint-like overlay coating, containing Ti and Mg oxides, performed best at both temperatures. Sputtered SiO_2 was effective at 450 °C but less so at 550 °C. Additionally, an alumina-based overlay coating was effective at 550 °C but less so at 450 °C. Specimen cracking and deformation during high-temperature exposure is also discussed.

1. Introduction

Rare-earth permanent magnets based on NdFeB or SmCo have high maximum energy products and find application in efficient motors and generators with high power to weight ratios. NdFeB-based magnets are cheaper than SmCo-based magnets and have superior magnetic properties at room temperature. However, due to a higher Curie temperature, at elevated temperatures SmCo-based magnets have superior magnetic properties. The highest temperatures at which NdFeB magnets can currently operate usefully is ~200 °C. By contrast, recently developed SmCo-based magnetic alloys can retain useful magnetic behaviour up to temperatures of ~550 °C [1,2], making them candidates for applications such as frictionless bearings or co-axial starter-motors/generators in gas turbine engines.

At elevated temperatures, oxidation of the rare-earth based magnets becomes a problem. In NdFeB-based magnets, it has been shown that degradation is due primarily due to the internal oxidation of the rare-earth element, creating an internal oxidation zone (IOZ) composed of a transition-metal-based matrix with the rare-earth oxide finely dispersed throughout [3]. The inward growth of this oxidation zone causes a loss of alloy volume with suitable microstructure for the desired permanent magnetic properties. In the case of SmCo-based magnets, the internal oxidation progresses extremely quickly [4–6] and, at the higher temperatures (500–600 °C), the oxidation zone can be millimetres deep after mere hundreds of hours of exposure. One solution to this problem is to give the alloy a protective coating, a strategy which is used extensively for high-temperature, long-lifetime components such as turbine blades, furnace elements and automotive exhaust catalyst supports. Saunders and Nicholls [7] review such coating strategies. Many of these techniques are intended for Fe- or Ni-based multicomponent alloys, and often rely on interactions between the surface layers and substrate. The concept of protective oxidation, which relies on deliberately forming a very dense and slow-growing oxide layer to block further ingress of oxygen can be achieved either by using surface layers rich in the appropriate element (e.g. Al or Cr) or may be side-stepped by using a ceramic coating composed of a protective oxide in a ready-formed state (e.g. silica).

The only work on protective coatings for SmCo magnets (that the authors are aware of) is a study by Chen et al. [8], who used electroplated Ni, electroless Ni and electrolytic Ag coatings between 8 and 23 μm thick at a temperature of 500 °C, with some success. In this current work the effectiveness of several speculative ceramic-based and metallic coatings, selected from those currently available for use by industrial turbine manufacturers for use in the engine hot sections, is investigated.

2. Experimental

Seven different coatings were applied to specimens of $Sm(Co_{0.74}Fe_{0.1}Cu_{0.12}Zr_{0.04})_{8.5}$. The specimens were approximately 10 mm × 10 mm × 2 mm in size with one set having the magnetic alignment (i.e. the *c*-axis of the crystals) in-plane and another set with alignment out of the plane of the specimen. The data for oxidation kinetics are referred to as either "parallel" or "perpendicular" which describes

* Corresponding author. Tel.: +44 0121 414 5172; fax: +44 0121 414 7468.
E-mail address: h.e.evans@bham.ac.uk (H.E. Evans).
[1] Deceased.

0925-8388/$ – see front matter © 2012 Elsevier B.V. All rights reserved.
doi:10.1016/j.jallcom.2011.12.031

Table 1
Coating systems used in this study.

Coating	ID	Thickness	Supplier
Sputtered SiO_2	A	<10 μm	Cranfield University
Electroplated Pt	B	1.5–5 μm on a 20 μm IOZ	TSTL
LR-1715A	C	5–10 μm	Indestructible Paints Ltd.
IP-9183-R1	D	~50 μm	Indestructible Paints Ltd.
IP-9029-R2	E	~50 μm	Indestructible Paints Ltd.
IP-9184-R2 (Khaki)	F	5–10 μm	Indestructible Paints Ltd.
PL-150-R1	G	30–40 μm	Indestructible Paints Ltd.

the relationship of the magnetic alignment and the IOZ growth direction. The coatings were applied to one side of the specimens only (on one of the large faces), partly for convenience but also in order for protected and unprotected surfaces to be compared directly under identical conditions. The sole exception was the electroplated Pt coating which was applied over the entire surface. The coatings are summarised in Table 1 where each variant is given a unique identification letter that will be used throughout the paper to identify a particular coating.

The silica coating (A), deposited by magnetron sputtering, was intended to act as an external diffusion barrier to the inward ingress of oxygen and would, thus, be expected to limit the depth of the IOZ. The coating formed was dense and adherent to the substrate alloy as can be appreciated from the cross-section shown in Fig. 1(a). The platinised variant (B) was an attempt to produce an internal diffusion coating rather than a simple overlay barrier. In this case, specimens were pre-oxidised for 4 h at 500 °C prior to coating in order to produce an internal oxidation zone approximately 20 μm deep, as determined by previous studies of oxidation kinetics [5]. The external oxides were then removed by light grinding. Following application of Pt, the samples were annealed for 1–4 h at 850 °C under vacuum in order to diffuse Pt into the Co-rich oxidation zone. Co and Pt form stable, corrosion-resistant phases and it was hoped that these interactions could produce a useful internal barrier layer. A cross-section of a coated specimen after the pre-oxidation and annealing treatment is shown in Fig. 1(b). The Pt coating shown here is the result of a 4-h anneal at 850 °C. It cans be seen that Pt has diffused through the entire depth of the pre-oxidised zone and begun to react with the underlying alloy, as evidenced by the thin layer of high-contrast columnar features extending a further 10 μm ahead of the main diffusion front.

The Indestructible Paints' coatings (C to G in Table 1) act as external overlay barriers and were applied either by spraying or painting. These are commercial coatings and detailed compositions were not made available although their nature can be understood from metallography and associated EDS analyses. Coating (C) is essentially Al-rich and appears dense and adherent but also shows some interaction with the underlying alloy (Fig. 1(c)). Coatings (D) and (E) are Al- and Si-rich with microstructures shown in Fig. 1(d) and (e). As can be seen in Fig. 1, each coating is multi-phase and each has again resulted in some interaction with the underlying alloy. Coating (F) is an inorganic paint-like coating, containing mainly Ti/Mg oxides, and used in industrial applications as a sealing barrier on Coating (D). There are no obvious interactions between Coating (F) and the alloy substrate (Fig. 1(f)). Coating (G) contains Si, Cr and K oxides used as a touch-up barrier coating. It is evident from Fig. 1(g) that the coating is cracked even in its as-received condition.

The highest temperature used in the application or formation of the coatings was for the platinising diffusion anneal at 800 °C. The specimens were cooled slowly after this anneal to replicate the final heat treatment stage of the magnets' production route. This was intended to ensure that the required cellular structure, consisting of cell walls based on the $SmCo_5$-type phase enclosing cells based on the Sm_2Co_{17}-type phase, was reproduced and that partitioning of Cu to the $SmCo_5$-type cell boundary phase [9,10] could also take place.

Specimens were oxidised in a similar manner to earlier studies [4,5], i.e. placed in alumina boats or tubes and exposed in laboratory air at temperatures of 450 °C and 550 °C for up to 600 h. These tests were isothermal, apart from the final cooling transient, and no attempt was made in the present work to examine the effect of repeated thermal cycling on coating endurance. After oxidation, the specimens were mounted in Quickset plastic, ground back by ~1 mm to give a cross-section perpendicular to their major faces using wet 120-grit SiC paper, further polished to 2400-grit on wet SiC and given a final polish using colloidal silica. They were examined using standard SEM/EDX techniques. The resulting internal oxidation zone thicknesses were measured at evenly spaced intervals along SEM images and averaged; the error on zone thickness is therefore the standard deviation of the individual measurements.

3. Results and discussion

3.1. Coating performance

Fig. 2 shows, at 450 °C (Fig. 2a) and 550 °C (Fig. 2b), internal oxidation zone thickness against time for the SiO_2-coated specimens (Coating A), in each case for both the coated and uncoated surfaces.

Fig. 2 appears to indicate that, although the SiO_2 coating offers good protection at 450 °C, there is only a slight improvement in

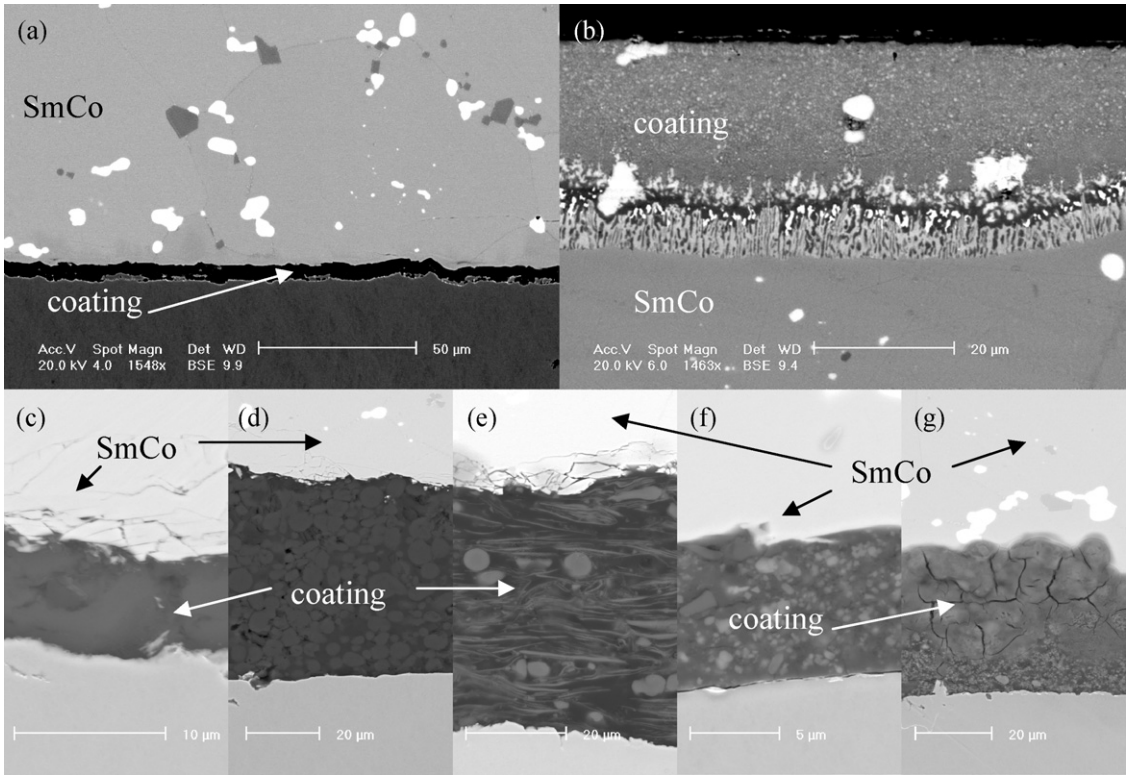

Fig. 1. Back-scattered electron (BSE) images of the various coating systems examined as listed in Table 1. The figures (a–g) refer to coatings A–G in sequence. In the case of (b), the outer surface is toward the top of the image; in all other cases the outer surface is toward the bottom of the image.

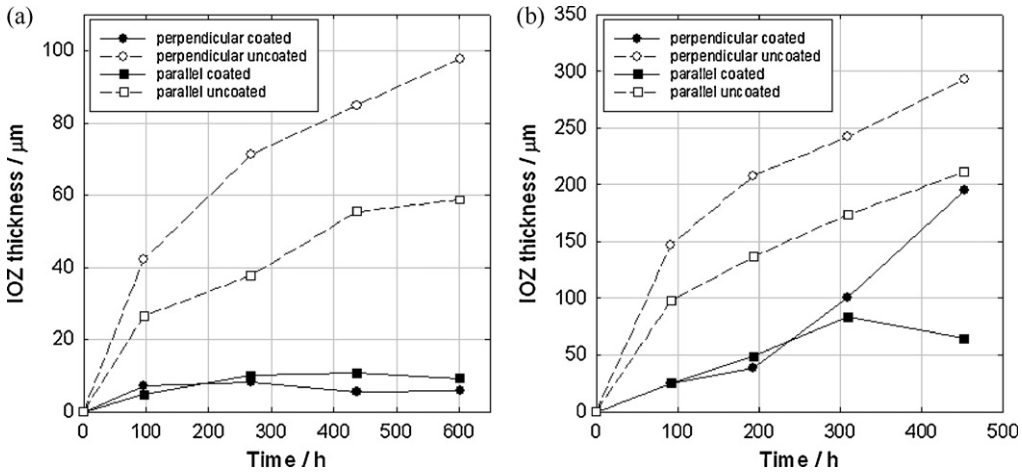

Fig. 2. IOZ thickness on SiO_2-coated specimens (Coating A) against exposure time for (a) 450 °C and (b) 550 °C. Parallel and perpendicular refer to the relative orientation of the magnetic alignment direction and the IOZ growth direction.

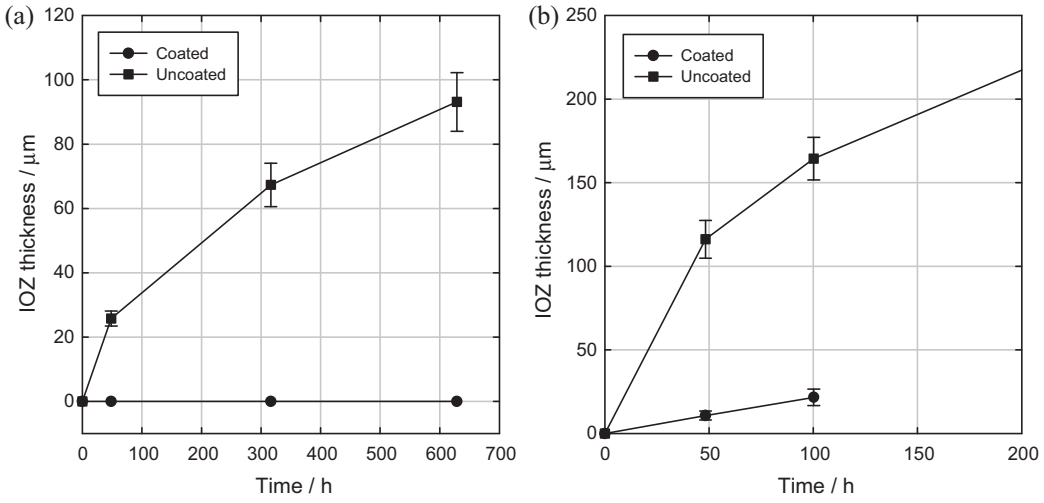

Fig. 3. IOZ thickness on Pt-coated specimens (Coating B) against exposure time for (a) 450 °C and (b) 550 °C. Measurements were made with the magnetic alignment direction perpendicular to the IOZ growth direction. The extended line for the uncoated specimens shown in (b) is not an extrapolation but links to an IOZ thickness measurement of 253 μm after an exposure of 268 h. This point is not shown on the graph to avoid excessive compaction of the horizontal axis.

corrosion behaviour at the higher temperature of 550 °C. However, the greater IOZ growth at 550 °C was frequently limited to regions immediately beneath small breaks in the SiO_2 layer. Away from these regions, IOZ growth was slower, more similar to the lower temperature behaviour.

Fig. 3 shows internal oxidation zone thickness against time for the Pt-coated pre-oxidised specimens (Coating B) and uncoated specimens exposed for the same times at temperatures of 450 and 550 °C. The Pt-coated specimens perform very well indeed. At 450 °C, there is no measurable internal oxidation beyond the pre-oxidised Pt-treated zone even after some 650 h. The 550 °C specimens have only been tested to 100 h, but here the Pt treatment is also effective.

Fig. 4 shows internal oxidation zone thickness against time for the Indestructible Paints' (IP) coated specimens (Coatings C to G), in each case for both the coated and uncoated surfaces and at both 450 and 550 °C. The uncoated values are measured on the same sample as the coated values; the error bars relate to statistical analyses of measurement of thickness at multiple points on a single specimen. Slight variations of IOZ growth rate for uncoated specimens in Fig. 4(a)–(e), nominally under identical conditions, are believed to be due to slight variations in environmental conditions during IOZ growth. It is immediately obvious that, for the IP coatings, Coating F is the best, providing complete protection at 450 °C and exceedingly good protection at 550 °C. Of the others, Coating C seems to provide the next best protection, being more protective, relative to the uncoated surface at the higher temperature of 550 °C. The other IP coatings all provide some degree of protection but not good enough to be useful at either temperature. It is interesting to note that the two most effective IP coatings were also the thinnest (5–10 μm) and least porous or cracked (Fig. 1).

Fig. 5 shows all the IOZ thickness curves (measured under faces perpendicular to the *c*-axis) collected together and compared with completely uncoated specimens, at both 450 and 550 °C. It is clear that all the coatings make some difference to the penetration of the internal oxidation front and they all perform better at the lower temperature of 450 °C than at 550 °C. The Pt coating (Coating B) and Coating F are almost 100% effective at 450 °C for up to 600 h of exposure but Coating A (silica) is only slightly less effective. At 550 °C, none of the coatings are 100% effective although Coatings B and F are still much better than the rest. In this case, however, Coating C is almost as protective as Coating F, both of them slightly better than Coating B. Coating A (silica) is almost as good but seems to fail after about 200 h, possibly because of cracking associated

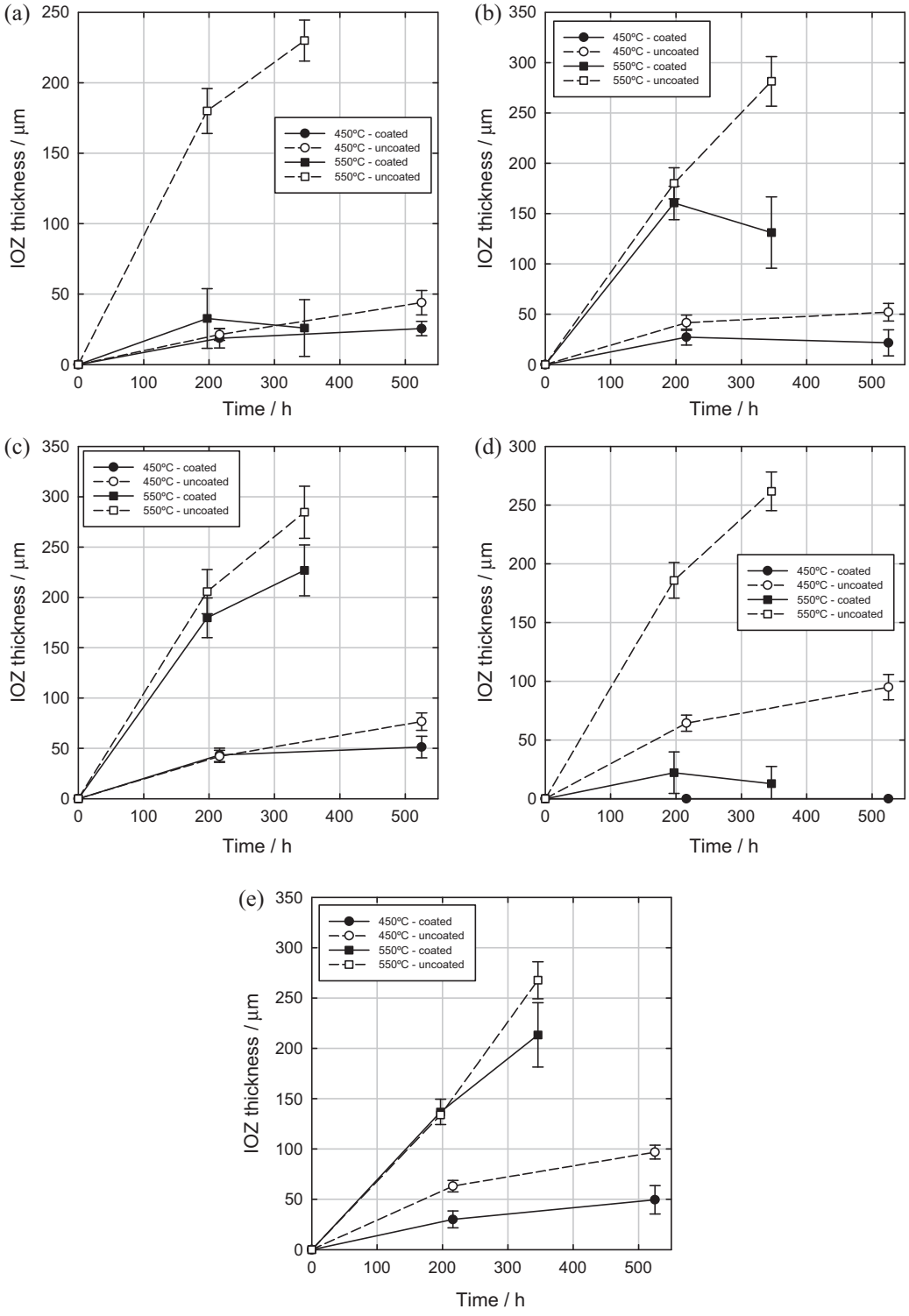

Fig. 4. IOZ thickness versus exposure time at both 450 °C and 550 °C for Indestructible Paints' coatings (Coatings C to G in Table 1, respectively). Measurements were made with the magnetic alignment direction perpendicular to the IOZ growth direction.

with IOZ development. The remaining coatings (D, E and G) make little difference to the penetration of the oxidation zone and offer no significant protection.

Comparison of these results with those of Chen et al. [8] is difficult because their coatings were assessed in terms of magnetic flux losses instead of oxidation zone penetration and at the intermediate temperature of 500 °C. However, magnetic flux losses can be assumed to be equivalent to the volume of the specimen occupied by the IOZ, which can be approximated as $A\Delta x$ where A is the surface area of the specimen and Δx is the IOZ thickness. From Fig. 5a, uncoated specimens at 450 °C suffer oxidation to a depth of ~90 µm after 600 h which, when multiplied by the specimen's surface area (10 mm × 10 mm × 2 mm ≡ 2.8×10^8 µm^2), gives a volume loss of ~12.5%. According to [8], the magnetic flux losses at 500 °C after 600 h are just under 12% which means that the volume approximation is good (it will slightly overestimate the volume due

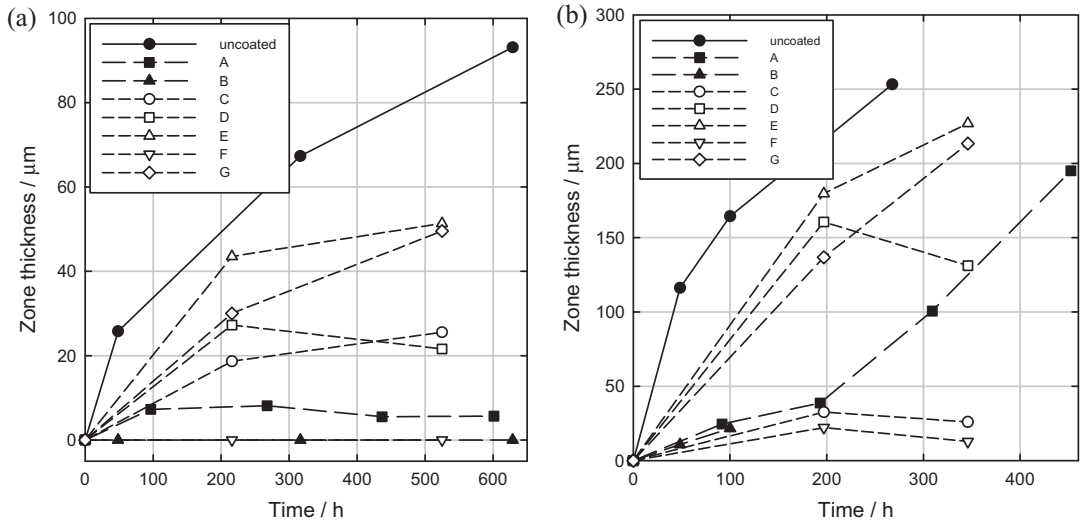

Fig. 5. IOZ thickness (measured in the perpendicular direction) versus time for the various coatings and an uncoated specimen, at (a) 450 °C and (b) 550 °C. Measurements were made with the magnetic alignment direction perpendicular to the IOZ growth direction.

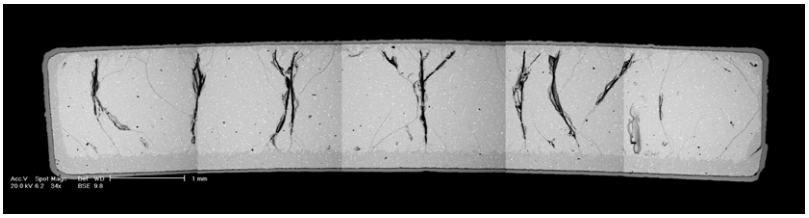

Fig. 6. Composite SEM image of a complete sample cross-section, exposed at 550 °C for 193 h. The specimen was coated only on the upper face of the specimen (as shown) with sputtered silica (Coating A).

to the specimen corners). Using the same approximations, the silica coating (Coating A) at 450 °C (Fig. 5a) gives almost exactly the same level of protection as the electrolytic Ni coating at 500 °C as measured by Chen et al. [8].

3.2. Specimen deformation and cracking

In none of the coating systems examined was there evidence of coating spallation on examination at room temperature after the cooling transient. Thermal cycling, as such, was not examined but this evidence suggests that all the coatings have reasonable mechanical stability.

The fact that some specimens were coated only on one major face caused the specimens to bend during exposure (see Fig. 6), such that the coated face became slightly convex. This would be expected if there were a volume decrease accompanying the phase changes caused by internal oxidation, since a greater volume of IOZ would now be forming under the uncoated face. However, assuming the reaction

$$Sm_2Co_{17} + (3/2)O_2 \rightarrow 17Co + Sm_2O_3$$

The volume change should be an increase of ~4%. This expansion accounts for the extensive through-section cracks observed in this grade of alloy, especially at longer times and higher temperatures [11], but not the observed bending effect. This is attributed to the difference in thermal expansion coefficients between the Sm_2Co_{17}-based substrate and the Co–Fe oxidation zone. For $Co_{25}Fe$, $\alpha = 13 \times 10^{-6}\,K^{-1}$ [12], whereas for Sm_2Co_{17}, $\alpha = 11.5 \times 10^{-6}\,°C^{-1}$ (perpendicular direction) and $9.5 \times 10^{-6}\,K^{-1}$ (parallel direction). The latter figures are available from the manufacturer's data sheets. Here there is a severe mismatch which results in the oxidation zone contracting ~30% more than the unaffected alloy upon cooling, which is likely to be the cause of specimen deformation. If the deformation does occur only during cooling, it is unlikely to affect the performance of the coatings except possibly when the furnace is opened during testing to remove specimens. Here the effect will be very small, since the observed temperature drop is typically less then 20 °C, for less than a minute.

4. Conclusions

Coating strategies already employed to protect mechanical components in high-temperature environments can also be used to protect Sm_2Co_{17}-based magnetic alloys up to 550 °C. The diffused Pt coating (Coating B), a paint-like overlay coating, containing Ti and Mg oxides (IP 9184-R1, Coating F) and the sputtered SiO_2 coating (Coating A) gave very good protection at 450 °C; this protection was complete in the case of the first two coatings. At the higher temperature of 550 °C, Coating B (diffused Pt) and (Coating F) were still the best, followed closely by an alumina-rich overlay (Indestructible Paints' LR-1715A, Coating C) and the SiO_2 coating (Coating A), although the protection was less effective. The efficacy of the various coatings was associated with a high density and absence of cracking.

Extensive through-section cracking observed in the unaffected alloy has been explained in terms of the volume expansion accompanying internal oxidation. The deformation observed on half-coated specimens has been explained in terms of the mismatch in thermal expansion coefficients between the oxidation zone and the original alloy.

Acknowledgments

This work was funded by the UK's Engineering and Physical Sciences Research Council (EPSRC) under grant reference EP/C518411/1. The authors would also like to thank Precision Magnetics Ltd. for supplying the alloy specimens, as well as Indestructible Paints Ltd., Turbine Surface Technology Ltd. (TSTL) and Cranfield University for supplying and applying the coatings.

References

[1] J.F. Liu, Y. Ding, Y. Zhang, D. Dimitar, F. Zhang, G.C. Hadjipanayis, J. Appl. Phys. 85 (1999) 5660.
[2] J.F. Liu, Y. Zhang, G.C. Hadjipanayis, J. Magn. Magn. Mater. 202 (1999) 69.
[3] Y. Li, H.E. Evans, I.R. Harris, I.P. Jones, Oxid. Met. 59 (2003) 167.
[4] W.M. Pragnell, A.J. Williams, H.E. Evans, J. Appl. Phys. 103 (2008) 07E127.
[5] W.M. Pragnell, A.J. Williams, H.E. Evans, J. Alloys Compd. 473 (2009) 389.
[6] S. Kardelby, A. Gebert, O. Gutfleisch, A. Handstein, U. Wyss, L. Schultz, IEEE Trans. Magn. 40 (2004) 2931.
[7] S.R.J. Saunders, J.R. Nicholls, Mater. Sci. Technol. 5 (1989) 780.
[8] C.H. Chen, M.Q. Huang, J.E. Foster, G. Monnette, J. Middleton, A. Higgins, S. Liu, Surf. Coat. Technol. 201 (2006) 3430.
[9] D. Goll, H. Kronmüller, H.H. Stadelmaier, J. Appl. Phys. 96 (2004) 6534.
[10] O. Gutfleisch, K.-H. Müller, K. Khlopkov, M. Wolf, A. Yan, R. Schäfer, T. Gemming, L. Schulz, Acta Mater. 54 (2006) 997.
[11] V. DePauw, D. Lemarchand, J.J. Malaridain, J. Magn. Magn. Mater. 172 (1997) 269.
[12] M. Takahashi, F. Ono, K. Takakura, AIP Conf. Proc. 29 (1976) 562.